Acta Astronautica 122 (2016) 1–9

Contents lists available at ScienceDirect

Acta Astronautica

journal homepage: www.elsevier.com/locate/actaastro

A satellite formation flying approach providing both positioning and tracking

Mark A. Nurge *, Robert C. Youngquist, Stanley O. Starr

Mail-Stop UBR3, National Aeronautics and Space Administration (NASA), Kennedy Space Center, FL 32899, United States

ARTICLE INFO

Article history:
Received 4 June 2015
Received in revised form
9 December 2015
Accepted 11 January 2016
Available online 19 January 2016

Keywords:
Spacecraft formation flying
Satellite swarms
Satellite propulsion
Satellite tracking
Satellite positioning

ABSTRACT

A magnetic field approach is presented whereby a large number of closely located satellites can be positioned and oriented relative to each other, but can also be tracked in six degrees of freedom. This is accomplished by using frequency-multiplexed magnetic fields where coils are placed on each satellite to allow them to generate magnetic fields, to interact with the magnetic fields from other satellites, and to sample the surrounding magnetic fields. By doing this, a satellite can choose which alternating field to push or pull against, to provide torque about, or to sample in order to determine its location and orientation relative to the other satellites. Theory is provided demonstrating the capability of this approach along with its advantages and limitations. An experimental system allowing 3 degrees-of-freedom was constructed and used to demonstrate a feedback and control system where a satellite is told to move to a location and it does this by interacting with the surrounding satellites to both generate forces and torques and to track its position and orientation.

1. Introduction

There is continued interest in developing close range satellite formation flying systems, or satellite swarms, as indicated by the demonstration of the Synchronized Position Hold, Engage, Reorient Experimental Satellites (SPHERES) project on the International Space Station [ISS] [1]. This system demonstrates an electromagnetic formation-flying concept developed over several years by MIT researchers [2–5] where coils on satellites produce constant magnetic fields whose dipole moments can be controlled. By adjusting the direction of the dipole moments in a cluster of satellites the orientation and position of the satellites can be controlled within the formation. However, due to the limited number of degrees of freedom in this approach, adjusting one satellite requires that all of the other satellites in the formation be adjusted as well, leading to control difficulties [6]. One way to alleviate this complexity is to frequency multiplex the magnetic fields produced by the satellites; a technique we described in a previous paper [7]. Each coil on each satellite can generate an oscillating magnetic field at a unique frequency so that it can produce synchronous oscillations with whichever other satellite coil it needs to interact, allowing it to yield the appropriate force or torque to achieve a given formation. This decouples the formation problem allowing forces and torques to be directed as desired throughout the swarm.

However, a satellite formation requires more than the production of forces and torques, it also requires a tracking and global communications system whereby each satellite knows its position and orientation relative to the other satellites in the formation. SPHERES uses an ultrasonic

* Corresponding author. Tel.: +1 321 861 9068.
E-mail addresses: Mark.A.Nurge@nasa.gov (M.A. Nurge), Robert.C.Youngquist@nasa.gov (R.C. Youngquist), Stanley.O.Starr@nasa.gov (S.O. Starr).

http://dx.doi.org/10.1016/j.actaastro.2016.01.010
0094-5765/

transmission system to provide position and attitude information [8], which is possible because SPHERES is operated within the air-filled portion of the ISS, but of course this approach will not work in the vacuum of space. Space applicable, relative navigation technology development for precision formation flying is called out in the NASA Roadmap on Communication and Navigation Systems [9]. Technologies such as image processing and laser rangefinders are suggested as possibilities, but image processing may not provide the accuracy needed for many applications and laser rangefinders become complicated and expensive when applied to a swarm with a large number of satellites.

In this paper, we describe an alternative relative navigation approach that uses the induced voltage in coils attached to satellites to determine their relative position and orientation. A key advantage of this approach is that it utilizes the same coils used to generate forces and torques, thereby minimizing additional structure to the formation of flying system. Also, significant redundant information is available, helping to ensure the reliability of this approach, but the key performance issue is whether the positional and angular resolution and accuracy that can be achieved with magnetic induction is sufficient. This will be discussed below. Then we will demonstrate a system where a mock-satellite, allowed to move in two dimensions and rotate about one axis, is located between four coils representing nearby satellites. In this system, forces and torques can be generated and the magnetic fields from the nearby satellites can be sampled to provide positional and angular information. The mock-satellite can be told to move to a given location and by using a feedback and control process, it determines how far it is from its goal and generates corresponding forces and torques to move to and then hold its position.

2. System operation description

In our previous paper [7], we showed that three linearly independent magnetic fields, each oscillating at a different frequency, were sufficient to generate the forces and torques needed to position and orient a satellite containing three orthogonal coils. We will not repeat that analysis here. However, we now need to verify that with the same coil configurations that sufficient information content is available to determine the position and orientation of the satellites as they move within the formation. With that in mind, we consider two different scenarios, both important to satellite formation flying. In the first scenario, it is assumed that multiple satellites must be positioned and oriented relative to a large nearby structure on which three reference coils can be located. This scenario would be useful for creating a large telescope where the mobile satellites would carry mirror elements. In the second scenario, the large reference coils are removed, leaving multiple identical mobile satellites that must track their location and orientation relative to the other satellites in the formation, i.e., a swarm. This scenario would be useful when a remote task, such as carrying a net to capture an asteroid, is required. These two cases are described below and in each case it is assumed that the mobile satellites contain three coils oriented along orthogonal planes.

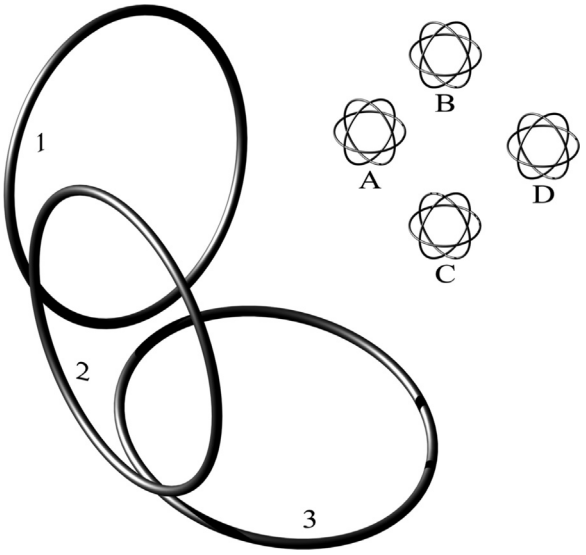

Fig. 1. By driving three reference coils, 1, 2, and 3, with currents at different frequencies, the position and orientation of the small mobile satellites relative to the large coils can be determined.

2.1. Reference coil case

Fig. 1 shows the reference coil case where three large coils, labeled 1, 2, and 3, are driven with a current oscillating at frequency f_1, f_2, and f_3, respectively. This creates three magnetic fields, $\vec{B}_i(x,y,z)\cos[2\pi f_i t+\phi_i]$, $i=1,2,3$, each oscillating at a different frequency and each being spatially independent from the other two at every location in space due to having distinct generating coils. We assume that these three magnetic fields are well known, either through measurement or through modeling, and due to the large size of the reference coils, that these magnetic fields have significant amplitudes throughout the space occupied by the small, mobile satellites; shown in Fig. 1 and labeled, A, B, C, and D. Each of these mobile satellites has three pick-up coils located on orthogonal planes and which will be indexed as $j=1,2,3$. Recall that Faraday's Law states that there will be an induced voltage in each of the mobile satellite coils caused by the change in magnetic flux passing through the area of the coil. So looking at satellite C, for example, there will be a set of induced voltages, $V_{Cij}(t)$, given by

$$V_{Cij}(t) = -\frac{\partial}{\partial t}\int_{\text{coil area},C_j} \vec{B}(x,y,z)\cos\left(2\pi f_i t+\phi_i\right)\cdot d\vec{A}_{Cj}$$
$$= 2\pi f_i \sin\left(2\pi f_i t+\phi_i\right)\int_{\text{coil area},C_j} \vec{B}_i(x,y,z,t)\cdot d\vec{A}_{Cj}. \quad (1)$$

Since the magnetic fields are spatially independent and the frequencies are not equal, the voltages, $V_{Cij}(t)$, obtained from the coils on satellite C represent nine independent measurements. Since position and orientation determination

require six degrees of freedom, these nine measurements provide more than enough information to track satellite C. The other mobile satellites, A, B, and D produce their own sets of nine voltages and can also fully determine their location and orientation relative to the three large coils.

2.2. Swarm satellite case

The swarm satellite case, as shown in Fig. 2, consists of a number, N (we will use the subscript $k=1,\ldots, N$ to index the individual satellites), of identical satellites. The three large reference coils are no longer present and this complicates the situation for two reasons; there is no longer a universal set of magnetic fields that the satellites can sample and the satellites are no longer coupled to a reference object. These two issues will be discussed below with two goals: (1) to provide enough information that the position and orientation of the satellites in the swarm can be known relative to the other satellites and (2) to provide information on the position and orientation of the entire swarm relative to some external object.

One might suggest that the satellites in the swarm can be tracked by choosing a single satellite and using it to supply the magnetic fields for the entire swarm, i.e., letting one satellite act as the three reference coils described in the preceding case. However, this is not feasible because

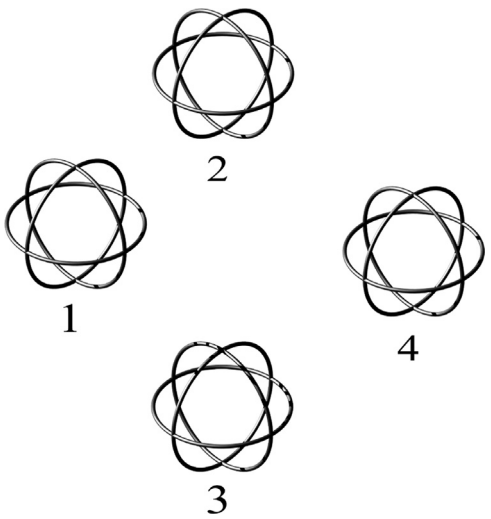

Fig. 2. By driving each satellite coil with a different frequency, nearest neighbors can determine their relative location and orientation. However, an independent system is needed to provide a total swarm position and orientation.

the relatively small size of the satellite coils limits the range over which its magnetic fields can be reliably sampled. Instead, we adopt a nearest neighbor approach. We drive an oscillating current through each satellites coils at frequencies, $f_{j,k}$, where $j=1,2,3$ indexes the three coils on each satellite number k. We set each of these $3N$ frequencies to different values so that there are $3N$ generated magnetic fields, each independent of both time and space from the others. Now assume that every satellite in the swarm is close enough to at least one other satellite that it can measure that satellites magnetic fields with its coils using Faraday's Law. That means, from the argument in the previous section, that each satellite can determine its position and orientation with respect to at least one other satellite in the swarm since it has nine independent measurements and only requires six. Assuming that all of the satellites in the swarm are connected through a nearest neighbor chain then all of the satellites in the swarm can track their position and orientation relative to all of the other satellites in the swarm. Quantifying this, the total minimum amount of information available to the swarm is greater than the total required degrees of freedom as

$$9N > 6(N-1). \tag{2}$$

Note that the total degrees of freedom required are $6(N-1)$ and not $6N$ because we are only determining the position and orientations of the satellites relative to each other. For example, if there are only two satellites all we can determine is the position of one relative to the other, i.e., 6 parameters. However, in order for a swarm to be useful its overall position and orientation must be known, for example, where is the swarm relative to a space vehicle or asteroid. Assuming that large reference coils are not an option, this global tracking requirement would need to be accomplished by some technique beyond that described in this paper, for example, image processing or laser tracking.

3. Resolution and accuracy

In our previous paper, we demonstrated that the magnetic forces between satellites could be controlled precisely enough to position mirrors on a future space telescope where a mirror element is attached to each satellite in the formation. The corresponding question in the present context is, “What is the resolution and accuracy of the position and attitude determination of the satellites using magnetic field sampling?” This is not an

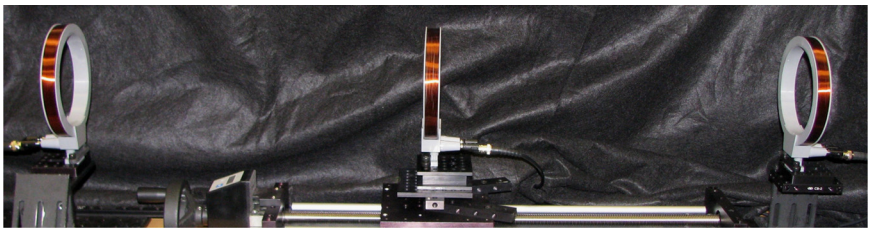

Fig. 3. Three aligned coils used to determine the resolution and accuracy of an idealized configuration representing one satellite located between two other satellites.

easy question to answer since it depends on the magnitudes and derivatives of the magnetic field components throughout space, so we have decided to address this by considering an idealized case. Assume that a satellite is located between two other satellites such that an identical coil on each satellite is aligned along a single axis, as shown in the experimental system in Fig. 3. The center coil is located on a translation stage allowing it to be moved along this axis while its induced voltage is monitored, simulating the motion of the center satellite between two outer satellites. The outer two coils are driven with the same frequency and current but with opposite phases so that the total magnetic field at the center location between them is canceled. Note that the two coils could be driven with different frequencies and the two center coil-induced voltage frequency components subtracted to obtain the same result, but using one frequency is simpler for this experiment.

The theoretical analysis of this experiment is useful because it shows how the performance of the system scales with various parameters. We have analyzed the system using elliptical integral expressions for the magnetic fields, see Appendix A [10], but the approximate far field magnetic field expressions are reasonably accurate and more clearly show the functional dependence. Using Lorrain and Corson [11] the far field magnetic induction along the axis of a coil with n current loops is

$$B = \frac{\mu_0 nI}{4\pi}\frac{2\pi a^2}{z^3}, \tag{3}$$

where $\mu_0 = 4\pi \times 10^{-7}$ N/A^2, I is the current in one loop, a is the coil radius, and z is the distance along the coil axis. If a coil is excited by a sinusoidal voltage with peak value, V_p, the peak current, I_p, induced in the coil is given by

$$I_p = \frac{V_p}{\sqrt{(2\pi f\, L)^2 + R_L^2}} \approx \frac{V_p}{2\pi f\, L}, \tag{4}$$

where f is the frequency of the drive voltage, L is the inductance of the coil, and R_L is the resistance of the coil. We chose to operate at a high enough frequency that $2\pi fL \gg R_L$ so that the approximation shown in Eq. (4) is valid. Another equation from Lorrain and Corson [11] provides an approximation for the inductance,

$$L = \mu_0 n^2 \pi a^2 K/d, \tag{5}$$

where d is the length of the coil and K is the Nagaoka coefficient [12], a dimensionless correction value that is approximately 1 for a long solenoid, $d \gg a$, and approaches 0 for a short coil, $d \ll a$. Combining Eqs. (3)–(5) yields an expression for the peak magnetic field,

$$B_p = \frac{d}{4\pi f\, z^3 n\pi K} V_p. \tag{6}$$

If only one of the outer coils in Fig. 3 has a voltage applied to it, then the peak induced voltage in the center coil, v_p, is found from Eqs. (1) and (6) to be

$$v_p = (2\pi f)(\pi a^2) n B_p = \frac{da^2}{2z^3 K} V_p. \tag{7}$$

This relatively simple expression relating the drive voltage on one satellite to the induced voltage on a second satellite shows that larger area coils respond better than smaller area coils. It is worth noting that this expression is independent of the drive frequency, which provides several advantages. Working at high frequency minimizes the power needed to drive the inductors due to the large inductive impedance. It allows frequencies to be selected where noise is minimal and where interference with other RF needs is eliminated. It also means that the induced voltages generated at different frequencies can be compared directly without performing frequency compensation.

Now, assume that the center coil in Fig. 3 is located a distance $z_0 + \Delta z$ from one outer coil and $z_0 - \Delta z$ from the other outer coil and assume that $\Delta z \ll z_0$. This models the situation where the center coil is located within a small region around the center point of the two outer coils. Recalling that the two outer coils are driven with opposite phases the peak voltage induced in the center coil is now the sum of the two outer coil effects. So from Eq. (7),

$$v_p = \frac{da^2}{2(z-\Delta z)^3 K} V_p - \frac{da^2}{2(z+\Delta z)^3 K} V_p \approx \frac{3da^2 V_p}{z_0^4 K}\Delta z. \tag{8}$$

This expression shows that the total induced voltage in the center coil varies linearly with position about the center point. The error in positioning the center coil is given by the derivative of this expression with respect to Δz and because this is linear the error is independent of position. Let Δz_r be the position resolution of the system, which is given by

$$\Delta z_r = \frac{z_0^4 K}{3da^2 V_p}\Delta v_p, \tag{9}$$

where Δv_p is the voltage resolution of the system, i.e., the error in the determination of the peak induced voltage in the center coil due to noise.

The coils used in the experiment each have 320 wraps of wire, a radius of 0.07 m and a thickness of 0.0175 m. Since the ratio of radius to thickness is 4, the Nagaoka coefficient, K, is equal to 0.24 [11,12]. The spacing between the outer coils in Fig. 3 is 1 m, so $z_0 = 0.5$ m. Using these values in Eq. (7) yields $v_p = 0.00143 V_p$, the inductance is calculated from Eq. (5) to be 0.027 H, and the change in peak voltage as the center coil is moved is 0.17 V/m from Eq. (8). These results are all approximately in agreement with experiment (to within 10%) indicating the functional dependencies shown are correct.

Using the more accurate elliptical integral expressions for the magnetic fields, we can calculate the induced voltage on the center coil as it is displaced over substantial distances and compare this with the experimental results (see Appendices A and B). The result is shown in Fig. 4 where we have used a coil inductance of 0.0245 H. Not only does the experimental data well match the theory, but both show a broad, nearly constant slope, region centered between the coils. This indicates that the result shown in Eq. (9) is approximately correct for a larger region than was indicated by the $\Delta z \ll z_0$ assumption. The presence of this large constant slope region makes this positioning approach attractive as a displacement sensor and it has been patented as such for both one-dimensional [13] and two-dimensional [14] cases.

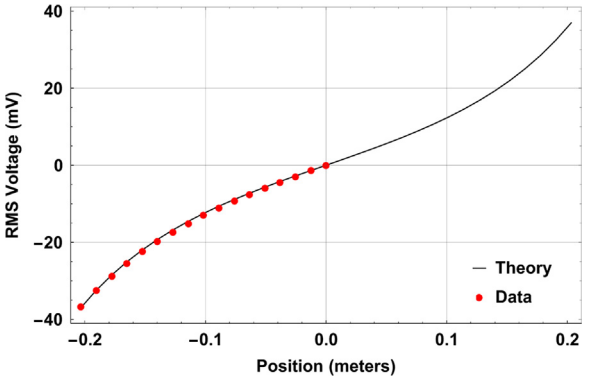

Fig. 4. Prediction versus theory for the induced RMS voltage of the system shown in Fig. 3 versus position of the center coil.

The experimentally determined slope at the center point is 0.117 V(RMS)/m when driving the outer coils with a 2 kHz sinusoidal 10 V peak voltage. Using a lock-in amplifier we measured the noise floor of the system as 0.4 $\mu V/\sqrt{Hz}$. This implies that the positioning resolution is 3.4 μm using a one-second integration time. By integrating over longer time periods, or modifying the coil parameters sub-micron resolution should be obtainable, which indicates that it might meet the requirements for mirror positioning in a future space telescope. In addition, the noise appears to be due to either test equipment limitations or background EMF being detected by the center coil, and is not due to the positioning system itself, so further resolution improvements may be possible.

Even though this positioning approach has excellent resolution, eddy current issues limit its accuracy. The presence of metal, i.e., conductive objects, causes eddy currents to flow and additional magnetic fields to be generated. Consequently, as the satellites move, their metallic parts cause the magnetic fields to be altered in ways that are difficult to track, and results in errors in accurately determining location. The magnitude and impact of this effect is difficult to estimate. In the case of a space telescope, once the mirrors are adjusted to yield an optimal focus the satellites are simply held in position and resolution, not accuracy, is the key issue. But in a swarm application where the satellites are moving significant relative distances, eddy current issues may limit the system performance to millimeter positioning accuracy instead of micron level performance.

As discussed in our previous paper, force and torque generation are accomplished by generating current in the coils, which requires the modulation frequencies be small such that $2\pi fL < R_L$. For the coils used in this paper the inductance is about 0.024 H and the resistance is about 6 Ω, so modulation frequencies less than 40 Hz would be optimal. However, as was shown in Eq. (7), the induced voltage in one coil is independent of the drive frequency in another coil. So the positioning system is independent of frequency and modulation frequencies in the kilohertz range reduce power requirements and allow the detection electronics to circumvent $1/f$ noise. Ideally, the coils are used in two different frequency bands, one low frequency band to generate forces and torques and one higher frequency band to generate the magnetic fields used for tracking the satellites.

4. Experimental demonstration of a feedback and control relative navigation system

An experiment was performed to demonstrate that magnetic coils could be used to both provide force and torque to a satellite as well as provide information on the location and orientation of the satellite. This experiment was not meant to optimize the performance of the approach, but to demonstrate feasibility. With that in mind, several design decisions were made that compromised the performance of the system, but that made the implementation of an operational system easier.

In space, the pseudo-forces on the satellites in the formation are primarily due to orbital variations; satellites further from the gravitational center move more slowly than those that are closer while two satellites at the same distance but having slightly different orbital inclinations will move toward and away from each other, completing one cycle per orbital period. So locally, these pseudo-forces can be of constant magnitude or can be oscillatory or some combination of these. Our simulator, using a freely hanging satellite, does not model either of these cases; instead modeling a spring type force that is dependent on the amount of twist felt by the string/wires attached to the mock-satellite. Consequently, even though we demonstrate in three-degrees-of-freedom that a satellite can be propelled, twisted, and tracked, this is in a system with known time constants (the oscillation periods of the hanging satellite due to induced torques). In any specific orbital case, there will be determinable pseudo-force magnitudes and time constants. The positioning system will need to account for these in order to overcome them as well as to not cause runaway oscillations.

The experimental system is shown in Fig. 5. Four coils were placed in fixed locations around a hanging coil assembly that represents the satellite. A double mobile configuration was used so that the satellite could move in two spatial dimensions and could rotate about one axis, modeling a three degree-of-freedom system. The satellite is shown in Fig. 6 and consists of four coils attached to a Plexiglas plate. Four coils were used instead of two in order to obtain a symmetric configuration and to simplify the system operation; instead of combining voltages at different frequencies on one coil we could separate signals onto different coils. The aluminum frame on the satellite is used to provide reference strips for a set of four laser rangefinders. The laser rangefinders, shown in Fig. 5 with the white cables, provided an independent measurement of the position and position stability of the satellite during operation of the system.

Fig. 7 is a circuit diagram for modeling a coil and its associated switching circuitry. The coil is represented as the sum of three components and a switching system is used to both drive current through the coil and to read its induced voltage. It would be preferable to use the coil for both force generation and magnetic field detection simultaneously, but the large drive voltage then appears along with the detection

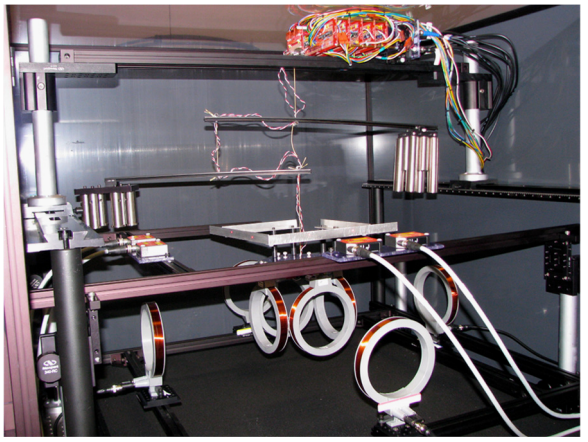

Fig. 5. The satellite was suspended using Kevlar string in a double mobile, allowing it to freely move in two spatial dimensions and rotate about an axis. Four fixed drive coils were used to provide frequency multiplexed magnetic fields corresponding to those produced by other satellites in the formation. The four laser rangefinders, shown with white cables attached, were used to independently track the motion of the satellite.

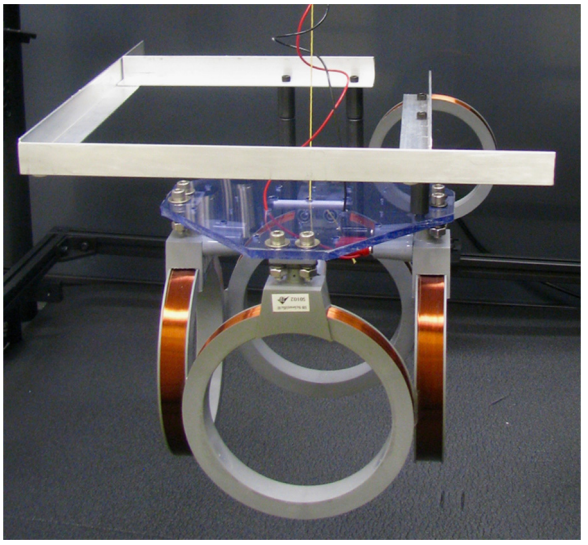

Fig. 6. A satellite simulator was composed of four coils attached to a Plexiglas plate. An aluminum frame was attached to this to provide a reflectance bar for the laser rangefinders.

signals and, even though it is in a different frequency band, its effects are difficult to remove. We made several attempts to isolate the drive and detection sections of the circuitry but always ended up with a reduction in power available when driving the coil. So we decided to use a pair of alternate state switches to separate the drive voltage from the detection voltage. We also ensured through the use of JFET op-amps that the detection voltage load resistor, R, was very large, minimizing the current draw through the coil during the detection period. Drawing current through the coil causes phase and amplitude shifts that degrade the system performance. With large R, the voltage output V is approximately equal to V_E. When the switches are in the opposite position of that shown in Fig. 7 it allows the coil to be driven with the

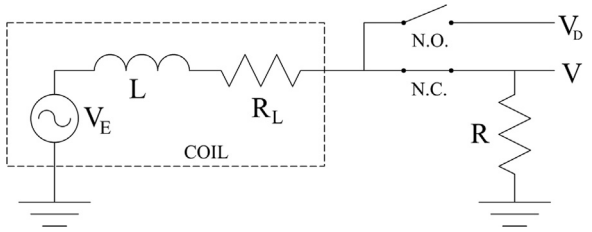

Fig. 7. A pair of switches are used to both monitor the induced voltage on a coil (V_E) and drive current through the coil (via V_D).

appropriate frequency waveform to generate the forces needed to change the location of the satellite.

We made a decision to operate the force/torque generation portion and the tracking system at the same frequencies. This was done in order to minimize the number of function generators used in the system and to allow the drive coils to be driven at single frequencies. Four dual channel function generators, shown in the system block diagram in Fig. 8, provided four primary drive signals at 270, 290, 310, and 330 Hz, one for each drive coil. The secondary channels were configured to provide a signal that was 180° phase shifted from each primary one. The outputs from the function generators were connected to the eight inputs on an 8×8 variable gain audio switch. The eight switch outputs were then routed to four dual-channel low impedance audio amplifiers to drive each coil with the proper frequency and phase. The switch was also used to route the desired primary or secondary signal to each of the four satellite coils and to coarsely vary its amplitude. When a drive and satellite coil face each other, an in-phase signal of the same frequency results in a repulsive force. Likewise, an out-of-phase signal results in an attractive force. A satellite coil that is approximately perpendicular to a given drive coil will cause the satellite to feel a torque when that individual coil is driven at the same frequency, where the phase relationship controls the direction of the torque.

The frequencies we selected are still low enough that substantial current can be forced across the coils against the inductive impedance, yet high enough that the induced voltages can be monitored with relatively low noise. The voltage V contains the frequency components of each of the surrounding drive coils and must be run through appropriate filtering to segregate the coupled signals. For this purpose, we constructed 16 custom lock-in amplifier circuits to monitor the voltage levels associated with four different drive frequencies on each of the four satellite coils. These circuits, coupled with the data acquisition system, required a few seconds to produce a low noise measurement. The forces are small, so the displacement of the satellite is small during the monitoring period, yet this does result in some error in the position measurement.

We can write down the equation for the voltages that the coil should see at a given location and orientation based on the equations in the appendices, but the challenge is to solve the resultant inverse problem. If we have multiple voltages from the various coils and frequencies on a satellite how do we find the position and orientation of the satellite? One

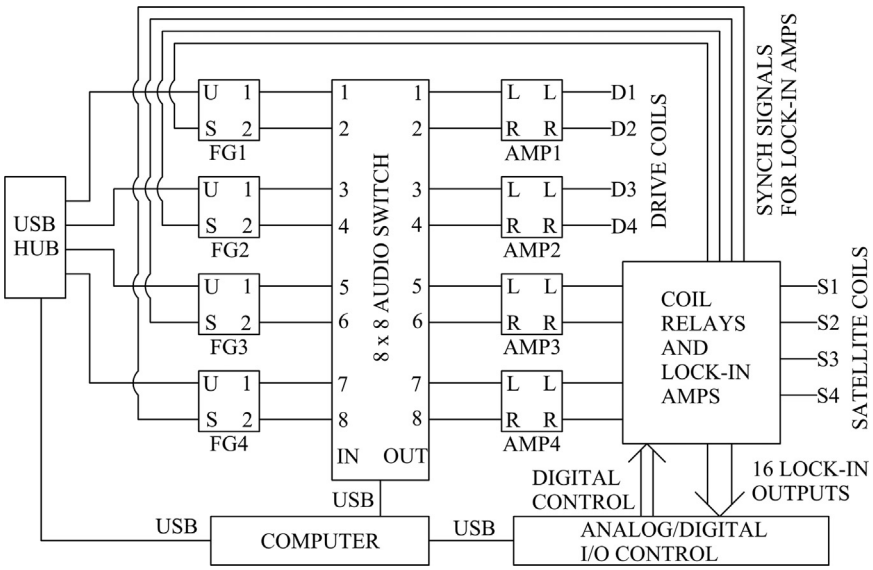

Fig. 8. A block diagram of the electronics configuration used for the system test. Four function generators (FG1–FG4) were used to generate the eight different drive signals. The 8×8 audio switch was used to apply the signal to the desired coil. The amplifiers provided the needed drive current and some custom build electronics used lock-in amplifiers and switches to read position from the four satellite coils.

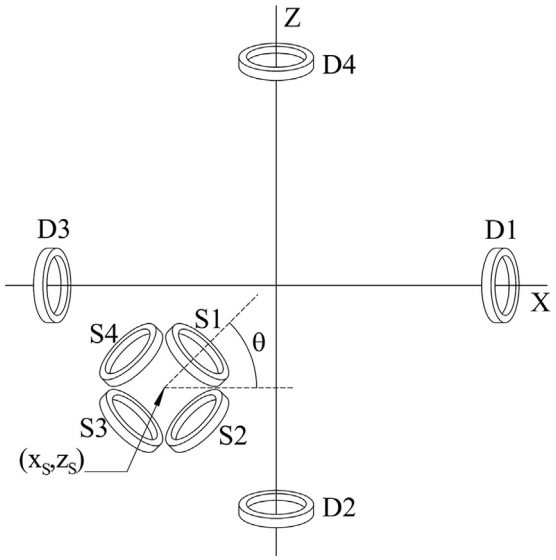

Fig. 9. This diagram shows the geometry and coordinate system used during testing. The voltage readings on the satellite coils were used to control determine the amount of feedback to apply based on differences with from a user selected set point. Four laser displacement sensors were used to track the satellite position (X_S, Z_S) and the rotation angle, θ. These measurements were used to track the satellite position and to determine how well it maintained position upon reaching the set point.

solution is to determine the voltages that the satellite will produce at a number of discrete locations and orientations. Then take the voltages from the satellite coils and find the best fit from a look up table and then perform a linear interpolation between nearby tabulated locations and orientations. We were able to demonstrate this using Mathematica, but a real-time version suitable for feedback and control was left for future implementation. The double mobile approach is not ideal; the force needed to move the satellite is dependent on the location of the counterweights and the string/wiring going to the satellite acts as a spring, which tries to return the satellite to a starting location. Even so, this approach is sufficient to demonstrate the concept and was relatively easy to implement. An enclosure was constructed around the experiment in order to minimize the effects of airflow.

Significant testing was performed with this system and a wide variety of feedback and control systems tested. Starting the satellite at a stationary location and orientation and telling it to move to a nearby location where the induced voltages were known yielded the best performance. By carefully choosing which induced voltages best represented displacement and which represented orientation, and by noting which drive current generated displacement forces and which generated torques, a complete feedback and control system could be demonstrated. Essentially, voltages proportional to the difference between the induced voltage at a current location and the induced voltages at the end location were fed back to the coils to push and twist the satellite into its desired position. An L2 norm of the differences was used to keep track of how close the satellite was to the final position and used to control the step size of the feedback.

To simplify things further, one quadrant of the system was used (see Fig. 9) with drive coils D2 and D3 set to push/ pull on satellite coils S2 and S3, respectively. Satellite coil S1 was used to control the torque from D2 to rotate the satellite. The four laser rangefinders were used to track the position (X_S, Z_S) and angle, θ, of the satellite and to evaluate how well the feedback and control system could maintain position once it reached the set voltages. Results for one of the control demonstration tests are shown in Fig. 10. For this test, the satellite coils alternated between 5 s drive and 2.5 s read periods. If the voltage difference between the set and read voltages was less than or equal to 0.015 V, the drive voltage was maintained at

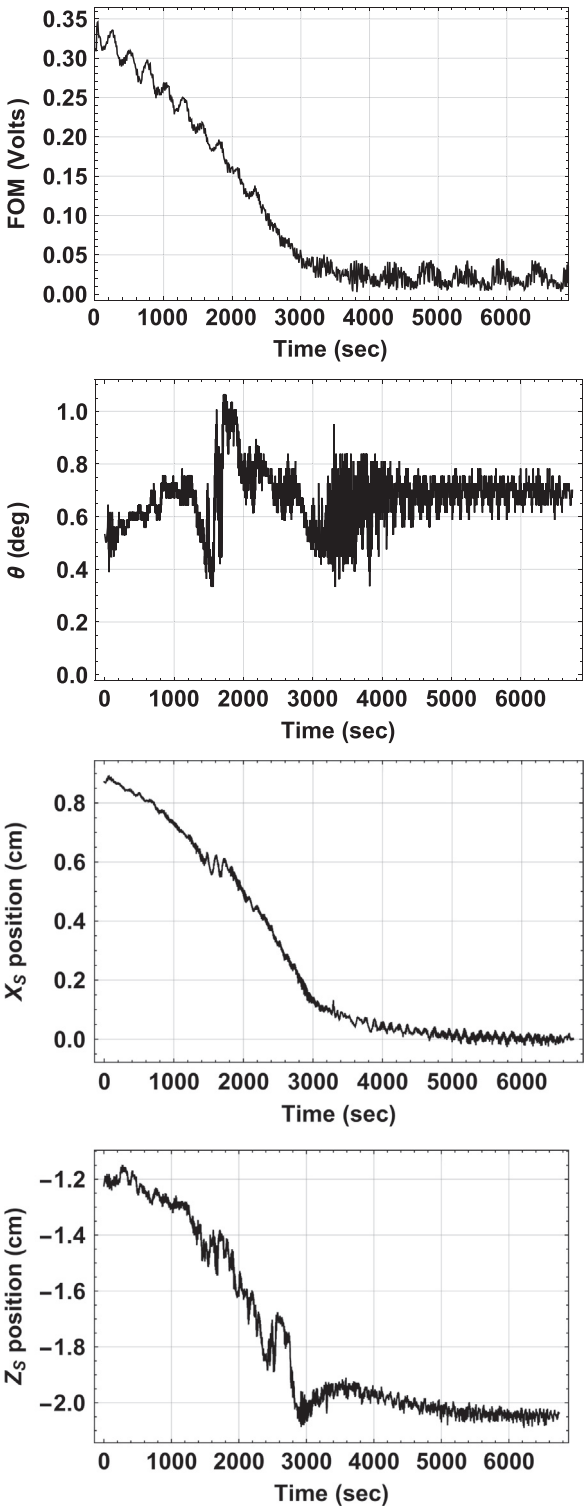

Fig. 10. Test results from a control demonstration test with alternating 5 s drive and 2.5 s read periods. The top plot shows the figure of merit based on the L2 norm of the difference between the set and read voltages. The other plots show the position of the satellite per Fig. 9.

the level used in the previous drive period. The plots show that the figure of merit was able to reach a level of approximately 0.02 V. The satellite angle moved approximately 0.2° and maintained position to within around $\pm 0.05°$. The position plots show that the satellite traversed about -0.9 cm in the x direction and around -0.9 cm in the z direction. The final position was held to within ± 0.025 cm.

5. Conclusions

We have demonstrated a relative navigation system for satellites flying in formations or swarms. The system relies on placing coils on each satellite and using these coils to generate modulated magnetic fields at different frequencies. This allows each satellite to monitor the induced voltages on its coils—sampling the frequency multiplexed magnetic fields—and using this to determine its position and attitude relative to the other satellites in the formation. We have shown that sub-micron position resolutions are possible using this approach, but that eddy current issues limit the accuracy of the approach. Even so, applications where the satellites are held in position, such as fixing the position and angles of the mirrors on a future multi-element space telescope, depend on resolution and not accuracy. The mirror's final optimal positions are determined by a focus adjustment process and after that they only need to be held. Other applications, such as controlling the motion of a swarm of satellites, may only require millimeter position accuracy and we have demonstrated that level of performance with a non-ideal experimental system. Future work in this area will be dependent upon choosing a specific application.

Acknowledgement

The authors would like to thank the NASA Space Technology Mission Directorate for providing funding for this study via the Center Innovation Funding Program.

Appendix A. Magnetic field components of a current loop

The magnetic field components for a current loop shown in Fig. A1 are given below in Cartesian coordinates [10]. The following substitutions are used for simplicity: $\rho^2 \equiv x^2+y^2$, $r^2 \equiv x^2+y^2+z^2$, $\alpha^2 \equiv a^2+r^2 2a\rho$, $\beta^2 \equiv a^2+r^2+2a\rho$, $k^2 \equiv 1\alpha^2/\beta^2$, $\gamma \equiv x^2y^2$, and $C \equiv \mu_0 I/\pi$. Note that ρ and r are non-negative. $E(k^2)$ and $K(k^2)$ are the complete elliptical integrals of the first and second kind, respectively:

$$f(x,y,z) = \frac{Cz}{2\alpha^2\beta\rho^2}\left[(a^2+r^2)E\left(k^2\right) - \alpha^2 K\left(k^2\right)\right]$$

$$B_x = xf(x,y,z)$$

$$B_y = yf(x,y,z)$$

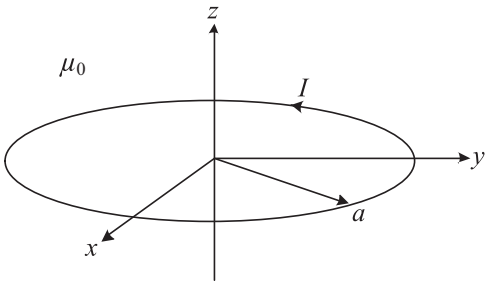

Fig. A1. Coordinate system for a current loop.

$$B_z = \frac{C}{2\alpha^2\beta}\left[(a^2 - r^2)E\left(k^2\right) + \alpha^2 K\left(k^2\right)\right] \tag{A.1}$$

Appendix B. Voltage pickup of a wire loop

The equation for the voltage pickup on a wire loop centered at (x_0, z_0) and at an angle θ to the drive coil is

$$V(x_0, z_0, \theta) = -\omega \int_{-a}^{a} \int_{-\sqrt{a^2-s^2}}^{\sqrt{a^2-s^2}} (B_x(s\ \cos\left[\theta\right] + x_0, y, s\ \sin\left[\theta\right] + z_0)\ \sin\left[\theta\right] + B_z(s\ \cos\left[\theta\right] + x_0, y, s\ \sin\left[\theta\right] + z_0)\ \cos\left[\theta\right])\, dy\, ds. \tag{B.1}$$

References

[1] E.M. Kong, A. Saenz-Otero, S. Nolet, D.S. Berkovitz, D.W. Miller, S.W. Sell, Spheres as a fromation flight algorithm development and validation testbed: current progress and beyond, in: The Second International Symposium on Formation Flying Missions and Technologies, 2004, pp. 14–16.

[2] E.M. Kong, D.W. Kwon, S.A. Schweighart, L.M. Elias, R.J. Sedwick, D. W. Miller, Electromagnetic formation flight for multisatellite arrays, J. Spacecr. Rockets 41 (4) (2004) 659–666.

[3] D.W. Miller, A. Saenz-Otero, J. Wertz, A. Chen, G. Berkowski, C. Brodel, S. Carlson, et al., Spheres: a testbed for long duration satellite formation flying in micro-gravity conditions, in: Proceedings of AAS/AIAA space Flight Mechanics Meeting, Clearwater, FL, 2000, no. AAS 00-110.

[4] D.W. Miller, R.J. Sedwick, E.M. Kong, S.A. Schweighart, Electromagnetic formation flight for sparse aperture telescopes, in: Aerospace Conference Proceedings, vol. 2, IEEE, 2002, pp. 2-729-2-741.

[5] S. Chintalapati, C.A. Holicker, R.E. Schulman, B.D. Wise, G.D. Lapilli, H.M. Gutierrez, D.R. Kirk, Update on spheres slosh for acquisition of liquid slosh data aboard the ISS, in: The 49th AIAA.ASME/SAE/ ASEE Joint Propulsion Conference, 2013, no. AIAA 2013-3903.

[6] X. Huang, C. Zhang, H. Lu, H. Yin, An LMI-based decoupling control for electromagnetic formation flight, Chin. J. Aeronaut. 28 (2) (2015) 508–517.

[7] R.C. Youngquist, M.A. Nurge, S.O. Starr, Alternating magnetic field forces for satellite formation flying, Acta Astronaut. 84 (2013) 197–205.

[8] S. Nolet, The spheres navigation system: from early development to on-orbit testing, in: AIAA Guidance, Navigation and Control Conference and Exhibit, 2007, pp. 20–23.

[9] J. Rush, D. Israel, C. Ramos, L. Deutsch, N. Dennehy, M. Seibert, Communication and Navigation Systems Roadmap, Technology Area 05, Technical Report Section 2.1.4 Position Navigation, and Timing, National Aeronautics and Space Administration, April 2012.

[10] J.C. Simpson, J.E. Lane, C.D. Immer, R.C. Youngquist, Simple Analytic Expressions for the Magnetic Field of a Circular Current Loop, NASA Technical Memorandum NASA/TM–2013-217919, National Aeronautics and Space Administration, New York, February 2001.

[11] P. Lorrain, D.R. Corson, Electromagnetic Fields and Waves, 2nd edition, . W. H. Freeman and Company, New York, 1970.

[12] H. Nagaoka, The inductance coefficients of solenoids, J. Coll. Sci. Imp. Univ. Tokyo Jpn. 27 (6) (1909) 1–33.

[13] R.C. Youngquist, S.M. Simmons, Inductive Position Sensor, US Patent 8,947,074 B1, February 2015.

[14] R.C. Youngquist, S.O. Starr, Two-Dimensional Inductive Position Sensing System, US Patent Application US2014266166 A1, February 2014.